2004

A SPLIT Model for Extraction of Subpixel Impervious Surface Information

Yeqiao Wang
University of Rhode Island, yqwang@uri.edu

Xinsheng Zhang

Citation/Publisher Attribution

Wang, Y. & Zhang, X. (2004). A SPLIT Model for Extraction of Subpixel Impervious Surface Information. *Photogrammetric Engineering & Remote Sensing*, *7*, 821-828. https://doi.org/10.14358/PERS.70.7.821
Available at: https://doi.org/10.14358/PERS.70.7.821

Creative Commons License

This work is licensed under a Creative Commons Attribution-Noncommercial-No Derivative Works 4.0 License.

A SPLIT Model for Extraction of Subpixel Impervious Surface Information

Yeqiao Wang and Xinsheng Zhang

Abstract

This paper introduces a Subpixel Proportional Land cover Information Transformation *(SPLIT) model to extract proportions of impervious surfaces in urban and suburban areas. High spatial resolution airborne Digital Multispectral Videography (DMSV) data provided subpixel information for Landsat TM data. The SPLIT model employed a Modularized Artificial Neural Network (MANN) to integrate multi-sensor remote sensing data and to extract proportions of impervious surfaces and other types of land cover within TM pixels. Through a control unit, the MANN was able to decompose a complex task into multiple subtasks by using a group of sub-networks. The SPLIT model identified spectral relations between TM pixel values and the corresponding DMSV subpixel patterns. The established relationship allows extrapolation of the SPLIT model to the areas beyond DMSV data coverage. We applied five intervals, i.e., <20 percent, 21 to 40 percent, 41 to 60 percent, 61 to 80 percent, and >81 percent, to map the subpixel proportions of land cover types. We extrapolated the SPLIT model from training sites that have both TM and DMSV coverage into the entire DuPage County with TM data as the input. The extrapolation received 82.9 percent overall accuracy for the extracted proportions of urban impervious surface.*

Introduction

Impervious surface is defined as any impenetrable material that prevents infiltration of water into the soil. Urban pavements, such as rooftops, roads, sidewalks, parking lots, driveways, and other manmade concrete surfaces, are among impervious surface types that featured the urban and suburban landscape. Impervious surface has been identified as a key environmental indicator due to its impacts on water systems and its role in transportation and concentration of pollutants (Arnold and Gibbons, 1996). Urban runoff, mostly through impervious surface, is the leading source of pollution in the Nation's estuaries, lakes, and rivers (Arnold and Gibbons, 1996; Booth and Jackson, 1997). Quantification of the percentage of impervious surface in a landscape has become increasingly important with growing concern over water quality in the U.S. (Civco *et al.*, 2002). Extraction of impervious surface information from remotely sensed data, particularly from Landsat TM or ETM+ data has been challenging because of mixed spectral information within the instantaneous-field-of-view (IFOV). In suburban areas, impervious surfaces are always mixed with tree canopies and other types of land cover at TM and ETM+ pixel level. Although 1 to 5 meter high spatial resolution remote sensing data are available, the data is usually expensive, particularly for large areas. Therefore, modeling approaches are in demand to integrate high spatial resolution remote sensing data with TM level data for extraction of subpixel information.

Yeqiao Wang is with the Department of Natural Resources Science, University of Rhode Island, Kingston, RI 02881 (yqwang@uri.edu).

Xinsheng (Kevin) Zhang was with the Department of Natural Resources Science, University of Rhode Island, Kingston, RI 02881; he is presently with EarthData International of Maryland, 7320 Executive Way, Frederick, MD 21704 (kzhang@earthdata.com).

Subpixel Classification

In remote sensing, the pixel is the minimum sampling unit. Classification of remotely sensed data assumes that a pixel represents a homogeneous land cover area. This assumption is often untenable with the pixels of mixed land cover composition (Foody, 1996). The mixed pixel problem can be well observed at the level of TM data in land cover mapping. The proportion of mixed pixels increases with a coarsening of spatial resolution of remote sensing systems (Townshend and Justice, 1981; Crapper, 1984; Irons *et al.*, 1985; Woodcock and Strahler, 1987). In remote sensing data acquisition, regardless of the effective resolution of a detector it is likely that the IFOV will intercept reflected energy from more than one land cover class since a solid-state detector integrates the intercepted radiance within the IFOV (Eastman and Laney, 2002). On the other hand, conventional classification algorithms cannot disaggregate individual land cover types that exist within the IFOV of sensor systems. Mixed pixels, restrictions of algorithms, the nature of fuzziness throughout training, and classification processes all limit the accuracy of information extraction from remote sensing data.

Numerous approaches have been developed to handle mixed pixel problems (Shimabukuro and Smith, 1991; Settle and Drake, 1993; Foody, 1994; Sohn and McCoy, 1997; Mayaux and Lambin, 1997; Ashton and Schaum, 1998; Grandell *et al.*, 1998). Considerable studies have been conducted to recover proportions of individual land cover types within the IFOV (Li and Strahler, 1985; Adams *et al.*, 1986; Roberts, *et al.*, 1993). Evaluations of methodologies that can be used to provide secondary labels at the resolution of polygons in vegetation mapping have been discussed (Woodcock *et al.*, 1996).

Three major approaches that have been investigated for subpixel classification include spectral mixture analysis, soft-classification procedures, and empirical approaches. The spectral mixture analysis (e.g., Settle and Drake, 1993; Bosdogianni *et al.*, 1997; Faraklioti and Petrou, 2000) determine the proportion of each constituent class by simulation equations which express the relationship between pixel reflectance and the unknown fractions of the land cover classes. This approach was considered with a limitation that the number

Photogrammetric Engineering & Remote Sensing
Vol. 70, No. 7, July 2004, pp. 821–828.

0099-1112/04/7007–0821/$3.00/0

of mixed classes that can be differentiated depends on the number of image bands (Eastman and Laney, 2002).

The soft-classification procedures estimate the degree of membership that each pixel has in each of the end-member classes. A Bayesian soft-classification applied mixed-cover training sites in a controlled experiment to estimate the underlying class signatures through the development of fuzzy mean reflectance and covariance matrices (Eastman and Laney, 2002). A maximum-likelihood approach and expert system rules were developed to estimate subpixel component of vegetation-impervious surface-soil in an urban land cover study using Landsat TM data (Hung and Ridd, 2002). The end product was a six-channel image in which each channel indicates a pre-defined ground component at the subpixel level.

The empirical approaches use models such as artificial neural network (ANN) to estimate area proportions. ANN has been applied in mixed-pixel handling (Foody, 1996; Moody *et al.*, 1996; Atkinson *et al.*, 1997; Foschi and Smith, 1997; Carpenter *et al.*, 1999). An empirical comparison between a modified maximum-likelihood classifier and a feed-forward backpropagation ANN in mapping continuous distribution of land cover indicates that the ANN classifier outperformed the maximum-likelihood classifier (Frizzelle and Moody, 2001). The ANN output exhibited stronger correspondence to class proportions for each class individually and for all classes and test regions combined. Another study suggests that the reliability of ANN as continuous classifiers might be improved by either transforming the output values of the ANN or by including mixed classes in the training data (Warner and Shank, 1997).

Among neural network applications, the backpropagation paradigm with a single-network-framed architecture is mostly adopted. It has been noticed that a single-network structure and the backpropagation algorithm may not be adequate to differentiate details among features that possess great spectral similarities (Wang and Civco, 1996), particularly in handling subpixel information from multiple sensors. It was suggested that certain network structures that were designed to learn analog patterns (Carpenter *et al.*, 1992) may produce superior results (Frizzelle and Moody, 2001). NeuralWare©, Inc. (1993) implemented a modular neural network architecture. The modularized architecture is to decompose a complex task into several subtasks. A modularized artificial neural network (MANN) consists of a group of local networks competing to learn different aspects of a problem. Each local network is an individual backpropagation network. A gating network controls the competition among subsets and learns to assign different regions of the data space to different local networks. MANN has been explored in multisource spatial data classification with improved accuracy (Wang and Civco, 1996). Software vendors have been developing subpixel processing capacity in their products (Flanagan and Civco, 2001).

With recent development in remote sensing data acquisition, a variety of high spatial resolution data is available for improved land cover mapping and information extraction (Lidov, *et al.*, 2000). However, since TM and ETM+ are the most widely applied data source in land cover mapping, challenges still remain in effective extraction of subpixel proportions of impervious surface and other types of land cover within TM pixels. In this paper, we present the Subpixel Proportional Land cover Information Transformation (SPLIT) model to differentiate proportions of land covers. We choose using MANN architecture for the SPLIT model with the hope that the MANN design can differentiate complex mixing scenarios of subpixel proportions. We focused on urban impervious surface, since it is among the most demanded information in environmental study and watershed management.

Method

Data Sources

This study used airborne digital multispectral videography (DMSV) data as the reference of subpixel information for the TM data. The DMSV data possesses two meter spatial resolution and has four spectral bands that are identical to the spectral coverage of the first four TM bands. The spatial relationship between DMSV and TM determines that 225 DMSV pixels (15 $\times$ 15) cover the same ground area as one TM pixel. The DMSV data in this study was acquired on 10 October 1997 for four selected sites in the DuPage County, Illinois (Plate 1a). Located in the west suburbs of Chicago, the landscape of the county is dominated by urban and suburban settings. A Landsat TM scene (Path 023/Row 031) on the same day of the DMSV data acquisition was available and purchased from the USGS EROS Data Center. The almost simultaneous data acquisition and identical selected spectral bandwidth between the two sensor systems made the set of DMSV data an ideal source of subpixel spectral information for the TM data (Plate 1). Since the DMSV data is available only for four selected sites in the county, extrapolation process is necessary to obtain subpixel information for the area beyond DMSV coverage by the SPLIT model.

The digital DMSV images were georeferenced to the state plane coordinate system and mosaicked. The TM data was geometrically rectified and georeferenced to the same coordinate system as the mosaicked DMSV imagery. The root mean square error of registration between the two data sets was 0.0043 TM pixels, or one DMSV pixel. In order to differentiate subpixel impervious surface from other land cover types, six general categories were applied which include *urban impervious surface*, *deciduous trees*, *coniferous trees*, *agricultural-land/grassland*, *wetland/water*, and *urban grass*. We conducted GPS-guided ground verification and recorded proportions of different land cover types in selected sampling sites. The obtained ground truthing locations served as references for selection of training data between DMSV and TM pixels.

SPLIT Model

The architecture of SPLIT model includes a MANN and a control unit. The MANN is a global network that consists of a group of simple-structured sub-ANNs, or subnets (Figure 1). MANN decomposes a complex task into multiple subtasks through the use of subnets. The subnets are assigned to learn different patterns of land cover proportions through a control unit. The number of subnets is the same as the number of output processing elements (PE). The control unit is designed to perform multiple functions that include: (1) task assignment; (2) inverse simulation of spectral features; and (3) decision and adjustment (Figure 1). The control unit includes a gate network and a supporting library that records all of the neural network parameters and the training patterns. During network training, the control unit and the supporting library learn the patterns of mixed land cover compositions, proportions, and the corresponding spectral features of the mixed pixels from the corresponding TM and DMSV pixel values. Once trained, the control unit will be able to screen the input data and subpixel patterns within the input, dissects the input, and distributes the input to the suitable subnet for further process. This design allows complex cases of subpixel patterns to be decomposed and effectively handled. For example, it was difficult to differentiate the proportions of land cover types that share certain similarities in spectral characteristics. A single-network framed ANN might perform poorly on differentiation of proportions among *agricultural/grassland* and *urban grass*. With MANN, the control unit detects the similarities among confusing categories and assigns the subnets that have been trained to handle these categories to extract the information.

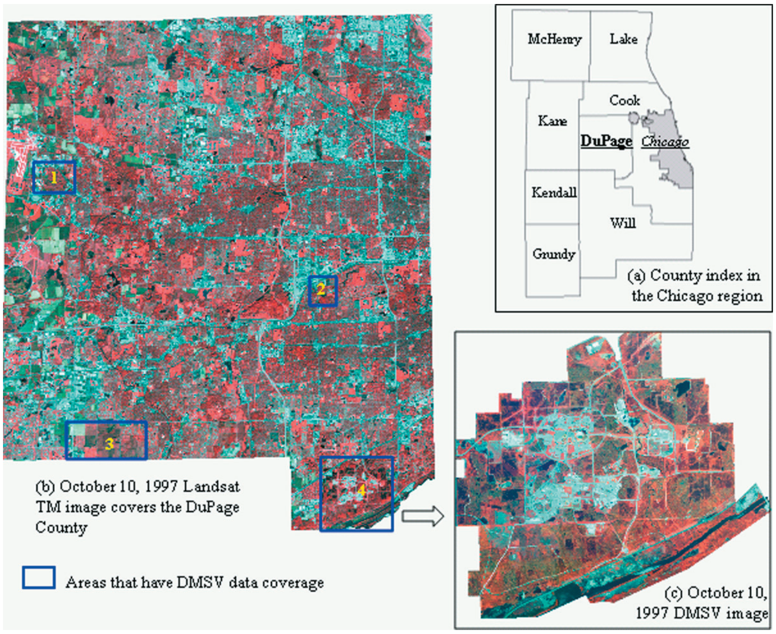

Plate 1. (a) The index map shows counties in the Chicago metropolitan region and the location of the DuPage County. (b) Landsat TM image of the DuPage County (band 4,3,2 in RGB) and the locations of four sites that have DMSV data coverage. (c) The example DMSV data shows the spectral similarities with TM and the finer spatial resolution.

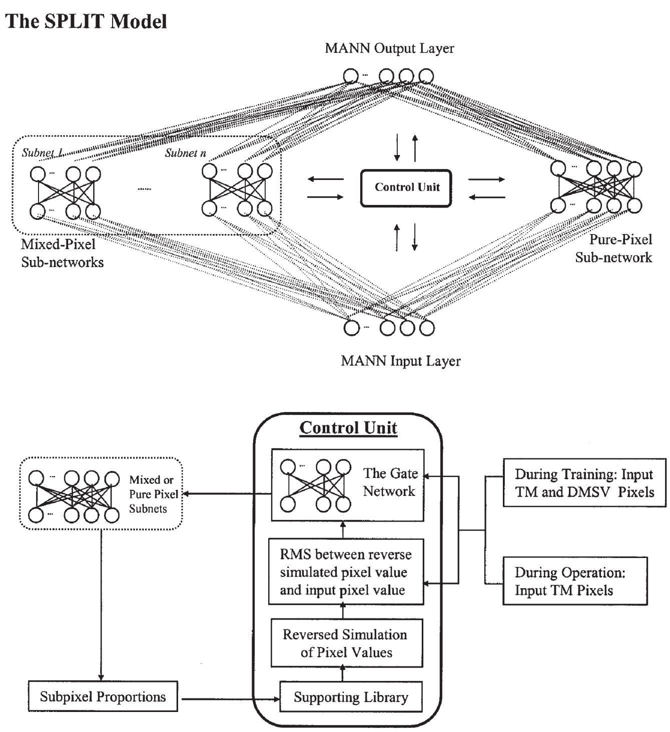

Figure 1. The SPLIT model consists of a modularized artificial neural network and a control unit.

Let L be the number of output processing elements (PE) of the control unit which is the same as the number of subnets, N as the number of MANN output which represents the level of proportions of land cover types, $y_k = (y_{k1}, \ldots, y_{kN})$ as the activation vector of k^{th} subnet output layer, $y = (y_1, \ldots, y_N)$ as the MANN output, and $c = (c_1, \ldots, c_N)$ as the activation vector of the output of the control unit. The output of l^{th} subnet is adjusted by c_l:

$$y = \sum_{l=1}^{L} c_l y_l. \tag{1}$$

MANN is trained by updating the weights connecting each of the PE. The update of the weights is derived by maximizing the objective function:

$$J = ln\left(\sum_{l=1}^{L} c_l e^{-0.5(d-y_l)^T(d-y_l)}\right) \tag{2}$$

where $d = (d_1, \ldots, d_N)$ is the desired output vector for the MANN. The quantity of h_k is used to describe the learning equations:

$$h_k = \frac{c_k e^{-0.5(d-y_k)^T(d-y_k)}}{\sum_{l=1}^{L} c_l e^{-0.5(d-y_l)^T(d-y_l)}}. \tag{3}$$

Standard backpropagation attempts to minimize a global error function E by:

$$-\frac{\partial E}{\partial I} = -\frac{\partial E}{\partial y}\frac{\partial y}{\partial I} = (d-y)\frac{\partial y}{\partial I} \tag{4}$$

where $I_k = (I_{k1}, \ldots, I_{kN})$ represents the pre-activation vector of k^{th} subnet output layer, and a standard quadratic error function is assumed. The corresponding values to backpropagation include (NeuralWare©, 1993):

- Backpropagate error for k^{th} subnet:

$$-\frac{\partial J}{\partial I_k} = -\frac{\partial J}{\partial y_k}\frac{\partial y_k}{\partial I_k} = h_k(d - y_k)\frac{\partial y_k}{\partial I_k}. \tag{5}$$

- Backpropagate error for k^{th} output PE of the control unit:

$$\frac{\partial J}{\partial s_k} = \sum_{l=1}^{L}\frac{\partial J}{\partial c_l}\frac{\partial c_l}{\partial s_k} = \sum_{l\neq k}\left(-\frac{h_1}{c_l}c_k c_l\right) + \frac{h_k}{c_k}(c_k - c_k^2)$$

$$= -c_k\sum_{l\neq k}h_l + h_k - c_k h_k = h_k - c_k\sum_{l=1}^{L}h_k = h_k - c_k. \tag{6}$$

Equations 5 and 6 indicate that the error at each subnet is weighted by its control unit.

In the training stage, the PE at the input layer accepts multispectral TM data and the corresponding subpixels of DMSV from the selected sample sites. Patterns of mixed land cover compositions, proportions, and corresponding characteristics of spectral features between the two data sets are recognized. The output layer of the MANN represents proportions of land cover types in TM pixels that are defined by subpixel patterns. In model operation, the input PE accepts TM data as the input. The control unit evaluates spectral patterns of the input and determines which subnet or a group of subnets should be assigned to handle the input data. For example, if a TM pixel is a mixture of two land cover types, one subnet that was trained to handle this composition will be assigned to process the input data. If there are three or more land cover types mixed in one TM pixel, the subnet that has been trained to handle the likely composition will be assigned to extract land cover proportions of the composition. Besides, the supporting library recorded spectral relations and similarities among land cover compositions. Therefore, closely related and confusing compositions can be better identified.

A pixel is considered *pure* if there is a dominant land cover type that accounts for over 80 percent of the TM pixel area. A *pure* pixel subnet (Figure 1) handles the pixels that have close to homogeneous subpixel spectral features.

The number of subnets depends on the number of considered compositions of mixed land cover types. Total number of possible compositions can be calculated by:

$$L = \sum_{i=2}^{n} C_n^i \qquad (i = 2, 3, 4, 5). \tag{7}$$

In Equation 7, n is the total number of land cover categories; i is the number of mixed land cover types within one TM pixel, and C_n^i is the number of possible compositions. We observed that most of the subpixel compositions were among two to five land cover types. The case of mixture of all six land cover types within one TM pixel was excluded because this composition was rarely observed. Since $n = 6$ and the considered compositions were among any two to five land cover types, the calculated L equals 56. Therefore, 56 subnets were imbedded into the MANN architecture. Each subnet was trained to handle one composition of mixed subpixels. The output of a subnet represents the proportions of that mixed land cover composition within the TM pixel.

Inversion Simulation

After initial extraction of subpixel proportions, the control unit performs an inverse transformation from proportion domain to spectral domain. The supporting library imbedded in the control unit supports the inverse simulation (Figure 1). The inverse transformation simulates spectral features of the TM pixel, i.e., pixel value (DN), based on obtained proportions of given land cover composition and on spatial aggregation pattern of subpixels. The purpose of inverse transformation is to examine the degree of similarity between the original spectral feature of TM pixel and the simulated spectral feature from proportions of land cover by DMSV data. The most likely composition and proportion of land cover types are determined by the root mean square error (RMSE) derived from inverse transformation:

$$RMS = \sqrt{\frac{\sum(b_i - \hat{b}_i)^2}{N}} \tag{8}$$

where N is the number of output PEs in an inverse subnet. b_i is the spectral value of i^{th} spectral band derived by the inverse simulation from the extracted proportions and land cover combinations from DMSV pixels; $\hat{b}_i$ is the pixel value observed from the TM. The RMSE is a measurement of closeness between simulated spectral features and the spectral value of the TM pixels. If the RMSE is greater than a threshold, the control unit will make an adjustment and reassign the job to another subnet that is the most relevant land cover composition for a new round of proportion extraction. Thresholds come from selected training samples in which the proportions of land cover types are known. The proportion extraction is accepted if the RMSE is lower than the threshold. If there is no subnet that can achieve a RMSE lower than the threshold, the output of the subnet that has the lowest RMSE will be saved.

Training and Testing Sample Selection

We conducted initial classifications on both TM and DMSV data to help in identification of the patterns of subpixel proportions and to establish relations between DMSV and TM pixels. We classified the TM and DMSV data into six land cover types. The locations of initial candidate training samples were selected from classified TM and DMSV data based on their land cover types. The selected sample locations were further compared with GPS-guided field checking results. This needs to point out that the initial classifications were to provide a background for possible sample locations and to facilitate training data selection. The real training data came from the selected TM pixels and the corresponding subpixels from DMSV data. The final selected training samples established the spectral relations between TM pixels and the corresponding DMSV pixels that act as subpixel information provider. It is the spectral characteristics of DMSV rather than the classification results that provide the subpixel pattern within the TM pixels.

We applied a moving window technique to extract sample of subpixel proportions of land covers from DMSV data. The window size was designed to represent the size of TM and multiple DMSV pixels. We selected 250 training samples for each case of the 56 mixed land cover combinations. Additional samples were selected by the same procedure and reserved for accuracy assessment. Figure 2 illustrates the procedures of training data selection. Plate 2 shows the examples of selected training sample locations and the comparison of mixed and pure pixels between the TM and DMSV data from the initial classifications.

Results

Since 225 DMSV pixels cover the same area as one TM pixel, the SPLIT model could potentially extract 1/225 of a TM pixel area as the minimum unit of subpixel proportions. For the purpose of subpixel proportional land cover mapping, we applied five generalized proportion intervals, i.e., 0 to 20 percent, 21 to 40 percent, 41 to 60 percent, 61 to 80 percent, and 81 to 100 percent. The trained SPLIT model was first applied to derive proportions of impervious surface and other types of

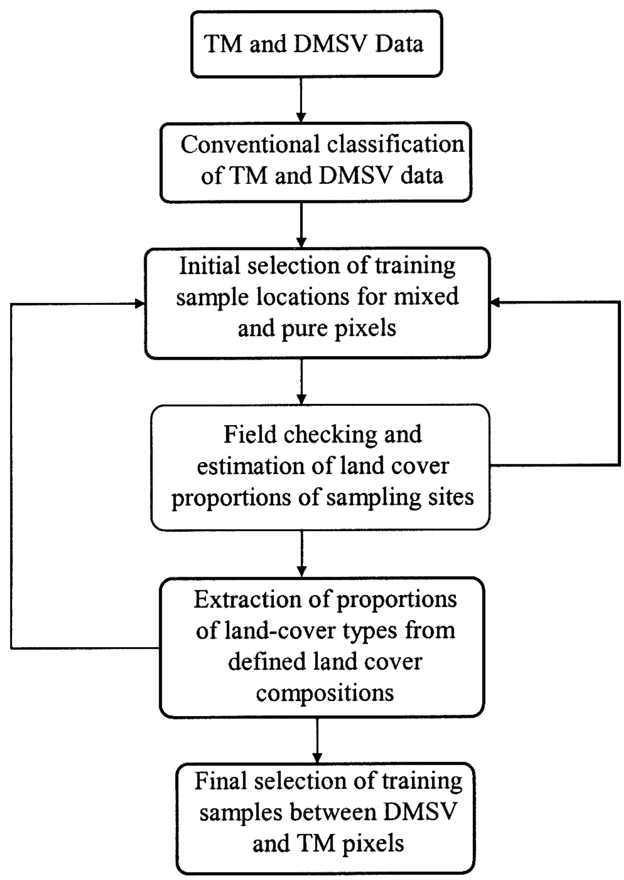

Figure 2. Procedures of selecting training samples to determine subpixel proportions of land cover types between DMSV and TM pixels.

land covers for the four sites that had DMSV coverage. Comparison between urban areas obtained from conventional classification of TM image (Plate 3a) and the subpixel proportions of urban impervious surface obtained from the SPLIT model (Plate 3b) shows that the subpixel proportions represent much more detailed information of impervious surface distribution than conventional classification of TM pixels. The TM pixels that cover continuous paved areas were identified at 80 to 100 percent proportions, while the narrow roads and edges of pavements were identified at lower proportions of urban impervious surface. Instead of using one fixed label for a classified TM pixel, the SPLIT model was able to extract subpixel proportions of land cover types within TM pixels.

With the trained SPLIT model and using TM data as the input, we extrapolated the extraction of subpixel impervious surface proportions beyond the DMSV data coverage into the entire DuPage County. The trained SPLIT model was able to differentiate the subpixel proportions of urban impervious surface based on spectral features of the input TM pixels (Plate 3c).

We conducted two separate accuracy assessments to evaluate the performance of the SPLIT model. We first applied an *average dynamic range* (ADR) to measure the correctness of proportion extractions for the areas that had DMSV data coverage. We used the reserved samples from GPS-guided ground truthing as the references to evaluate the correctness of SPLIT derived subpixel proportions. The ADR is defined as:

$$ADR = \sqrt{\frac{\sum_{i=1}^{n} \sum_{j=1}^{m} (p_{ij} - \hat{p}_{ij})^2}{n}} \qquad (17)$$

where, n is the total number of testing sites; m is the total number of land cover categories; p_{ij} is the SPLIT-derived value of proportions of the j^{th} land cover types in the i^{th} pixel; $\hat{p}_{ij}$ is the value of the observed proportion of the j^{th} category in the i^{th} pixel in DMSV. The larger the ADR value, the lower the accuracy of proportion extraction. The ADR values indicate that proportions of land cover types can be more accurately simulated when fewer land cover types exist within one TM pixel (Table 1). Less number of land cover types within a mixed pixel reduces the complexity of land cover composition so that the extracted proportion can be more accurate. The SPLIT model worked most effectively on the combinations of two land cover types within a TM pixel. The ADR value increased when there were more land cover types mixed within TM pixels. The SPLIT model performed well when the proportion level is between 41 to 60 percent. Higher ADR values were observed at the 21 to 40 percent and 61 to 80 percent proportion intervals. The reason could be that there was no dominant proportion of land cover types at the middle ranged mixing proportions (41 to 60 percent). Therefore, the relationships between TM pixel values and the mixing patterns of DMSV subpixels could be more accurately identified and extracted. When the proportion intervals were off the middle ground, i.e., at 21 to 40 percent and 61 to 80 percent intervals, the influence from one dominant land cover type could reduce the effectiveness of extracting proportions of other land cover types within the TM pixels. The 81 to 100 percent interval was considered as a pure pixel and these pixels were handled by the pure pixel subnet. We evaluate the SPLIT performance on pure pixel by sample-based accuracy assessment (e.g., Table 2) rather than by ADRs.

After the extrapolation of SPLIT model to the entire DuPage County, we conducted an accuracy assessment through ground verification across the county for the proportions of impervious surface. The result in Table 2 indicates that the higher the proportions of impervious surface area

TABLE 1. THE AVERAGE DYNAMIC RANGE (*ADR*) OF LAND COVER PROPORTIONS IN DIFFERENT INTERVALS

Number of Land Cover Types in a Mixed TM Pixel	Number of Test Sites	ADR in Different Proportion Interval				Overall ADR (%)
		0–20 (%)	21–40 (%)	41–60 (%)	61–80 (%)	
2	350	7.85	9.05	5.22	8.22	8.77
3	255	7.89	8.65	5.16	10.67	9.39
4	150	10.12	11.22	8.71	10.98	10.42
5	70	11.25	12.35	8.91	12.82	11.56

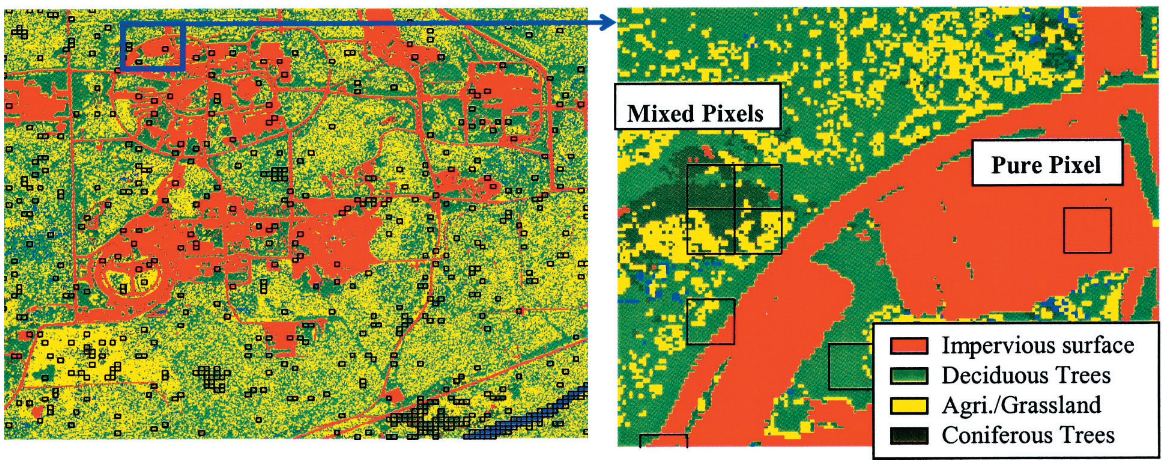

Plate 2. Locations of training samples and examples of pure and mixed subpixel information within the TM pixel areas.

TABLE 2. ACCURACY ASSESSMENT OF SPLIT MODEL DERIVED PROPORTIONS OF IMPERVIOUS SURFACE

	SPLIT Model Derived Proportions of Impervious Surface							
Reference	0–20%	21–40%	41–60%	61–80%	81–100%	Row Total	Omission Error	Accuracy
0–20 %	154	30	7	1		192	19.79%	80.21%
21–40%	28	182	10	3	1	224	19.91%	81.25%
41–60%	16	7	173	10	2	208	16.83%	83.17%
61–80%		2	24	164	6	196	16.33%	83.67%
81–100%				10	88	98	10.20%	89.79%
Column Total	198	221	214	188	97	918		
Commission Error	22.22%	17.67%	19.16%	12.77%	9.28%			Overall 82.90%

within a TM pixel, the better the accuracy achieved. The high-end intervals are either close to or among the pure pixels. The pure pixels at 80 to 100 percent interval achieved the best accuracy. The 41 to 60 percent and 61 to 80 percent proportions achieved about the same accuracy in extraction of urban impervious surface.

We also applied the SPLIT model to extract proportions of other types of land covers. Plate 3d shows the result of extracted subpixel proportions on deciduous trees. It demonstrates that the SPLIT model is capable of extracting different types of subpixel proportions as long as the training samples are available.

Discussion

This study explored a modeling approach of using multisensor remote sensing data to extract subpixel proportions of land cover information. The SPLIT model successfully extracted the proportions of urban impervious surface in a study area that has predominately suburban residential and commercial landscape. Instead of using a fixed label of land cover type for classified TM pixels, subpixel proportions of land covers provide additional detailed information for the TM pixel locations. Several factors contributed to the performance of the SPLIT model.

First, the identical spectral coverage between the DMSV, and the first four bands of TM is the basic requirement to establish the relationships between spectral features of TM pixels and the DMSV, subpixel spectral patterns. The study shows that TM and DMSV data are among the reliable data sources to be integrated in extraction of subpixel land cover proportions. In addition, the same day and almost simultaneous data acquisition of TM and DMSV data assured the quality of the subpixel information. Otherwise, appropriate image processing such as histogram matching will have to be conducted to match coarser resolution sensor data with finer resolution subpixel information providers.

Secondly, the SPLIT model consists of a modularized artificial neural network and a control unit. This mechanism was able to decompose a complex task, such as complex mixing scenarios of subpixel proportions, into simplified subtasks with specific targets of land cover compositions and proportions. The subnets are capable of obtaining reliable information about proportion compositions.

Thirdly, the inverse simulation reinforced the evaluation of the closeness of extraction of land cover proportions. This process assured the accuracy of subpixel information extraction since it adopted the combination of land cover types and the proportion intervals that most closely matched the original TM pixel values.

Furthermore, the supporting library imbedded within the control unit recorded the patterns between TM pixel features and the DMSV subpixel compositions during the training process. Once trained, the SPLIT model can be extrapolated to the areas that have no finer spatial resolution data coverage by

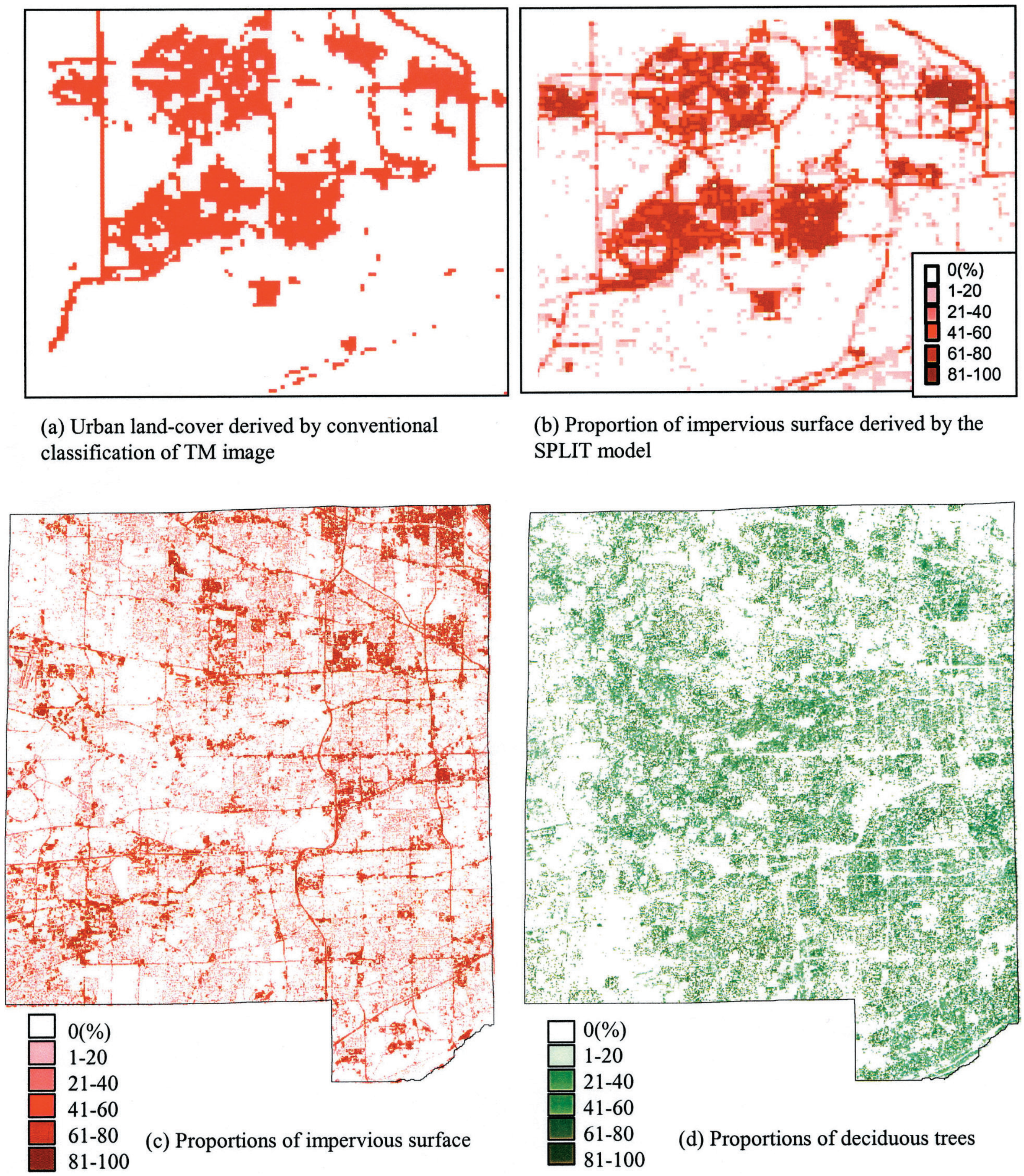

Plate 3. The comparison of urban land cover and proportions of urban impervious surface areas derived by conventional classification of TM (a) and by the SPLIT model (b). The results of extrapolation of SPLIT model into the entire DuPage County for extraction of subpixel proportions of urban impervious surface (c), and subpixel proportions of deciduous trees (d).

simulation operations. Therefore, the SPLIT model is an effective way of using limited resources of high spatial resolution data to obtain extended subpixel proportions for a large area. The model works well for extraction of impervious surface information in suburban settings where mixed pavements and woodland are common in residential areas. This approach can be applied to integrate data from other multiple sensors for subpixel information extraction as well.

Acknowledgments
This research was funded by the National Aeronautic and Space Administration (Grant No. NAG5-8829). The authors wish to express thanks to Leslie Berns and Wayne Lampa for their guidance in ground truthing and verification. The Chicago Biological Council (*a.k.a., Chicago Wilderness*) funded the DMSV data acquisition in a separate project. The authors appreciate the comments and critiques from three

anonymous reviewers that helped greatly in improvement of the manuscript.

References

Adams, J.B., M.O. Smith, and P.E. Johnson, 1986. Spectral mixture modeling: A new analysis of rock and soil types at the Lander 1 site, *Journal of Geographical Research*, 91:8098–8112.

Arnold, C.A. Jr., and C.J. Gibbons, 1996. Impervious surface coverage: the emergence of a key urban environmental indicator, *Journal of the American Planning Association*, 62(2):243–258.

Ashton, E.A., and A. Schaum, 1998. Algorithms for the detection of subpixel targets in multispectral imagery, *Photogrammetric Engineering & Remote Sensing*, 64:723–731.

Atkinson, P., M. Cutler, and H. Lewis, 1997. Mapping subpixel proportional land cover with AVHRR imagery, *International Journal of Remote Sensing*, 18:917–935.

Booth, D.B., and C.R. Jackson, 1997. Urbanization of aquatic systems: Degradation thresholds, stormwater detection, and the limits of mitigation, *Journal of American Water Resources Association*, 35(5):1077–1090.

Bosdogianni, P., M. Petrou, and J. Kettler, 1997. Mixture models with higher order moments, *IEEE Transactions on Geoscience and Remote Sensing*, 35(2):341–353.

Carpenter, G.A., S. Gopal, S. Macomber, S. Martens, C.E. Woodcock, and J. Franklin, 1999. A Neural Network Method for Efficient Vegetation Mapping, *Remote Sensing of Environment*, 70:326–338.

Carpenter, G.A., S. Grossberg, N. Markuzon, J.H. Reynolds, and D.B. Rosen, 1992. Fuzzy ART: A neural network architecture for incremental supervised learning of analog multidimensional maps, *IEEE Transactions in Neural Networks*, 3:698–713.

Civco, D.L., J.D. Hurd, E.H. Wilson, C.L. Arnold, and S. Prisloe, 2002. Quantifying and Describing Urbanizing Landscapes in the Northeast United States, *Photogrammetric Engineering & Remote Sensing*, 68(10):1083–1090.

Crapper, P.F., 1984. An estimate of the number of boundary cells in a mapped landscape coded to grid cells, *Photogrammetric Engineering & Remote Sensing*, 50:1497–1503.

Eastman, J.R., and R.M. Laney, 2002. Bayesian Soft Classification for Sub-Pixel Analysis: A Critical Evaluation, *Photogrammetric Engineering & Remote Sensing*, 68:1149–1154.

Faraklioti, M., and M. Petrou, 2000. Recovering more classes than available bands for set of mixtured pixels in satellite images, *Image and Vision Computing*, 18:705–713.

Flanagan, M., and D.L. Civco, 2001. Software Review: Imagine Subpixel Classifier Version 8.4, *Photogrammetric Engineering & Remote Sensing*, 67:23–28.

Foody, G.M., 1994. Ordinal-level classification of subpixel tropical forest cover, *Photogrammetric Engineering & Remote Sensing*, 60: 61–65.

Foody, G.M., 1996. Relating the Land-Cover Composition of Mixed Pixels to Artificial Neural Network Classification Output, *Photogrammetric Engineering & Remote Sensing*, 62:491–499.

Foschi, P.G., and D.B. Smith, 1997. Detecting subpixel woody vegetation in digital imagery using two artificial intelligence approaches, *Photogrammetric Engineering & Remote Sensing*, 63:493–500.

Frizzelle, B., and A. Moody, 2001. Mapping continuous distributions of land cover: A comparison of maximum-likelihood estimation and artificial neural networks, *Photogrammetric Engineering & Remote Sensing*, 67(6):693–705.

Grandell, J., J. Pulliainen, and M. Hallikainen, 1998. Subpixel land use classification and retrieval of forest stem volume in the boreal forest zone by employing SSM/I data, *Remote Sensing of Environment*, 63:140–154.

Hung, M.C., and M.K. Ridd, 2002. A sub-pixel classifier for urban land-cover mapping based on a maximum-likelihood approach and expert system rules, *Photogrammetric Engineering & Remote Sensing*, 68:1173–1180.

Irons, J.R., B.L. Markham, R.F. Nelson, D.L. Toll, and D.L. Williams, 1985. The effects of spatial resolution on the classification of Thematic Mapper data, *International Journal of Remote Sensing*, 6:1385–1403.

Legendre, P., 1993. Spatial Autocorrelation: trouble of new paradigm? *Ecology*, 74:107–138.

Li, X., and A.H. Strahler, 1985. Geometric-optional modeling of a conifer forest canopy, *IEEE Transactions on Geoscience and Remote Sensing*, GE-23:705–721.

Lidov, L., R. Miller, D.M. Wormer, and K. Tilley, 2000. Understanding the future of commercial remote sensing, *Photogrammetric Engineering & Remote Sensing*, 66:3–12.

Mayaux, P., and E.F. Lambin, 1997. Tropical forest area measured from global land-cover classifications: inverse calibration models based on spatial textures, *Remote Sensing of Environment*, 59: 29–43.

Moody, A., S. Gopal, and A.H. Strahler, 1996. Sensitivity of neural networks to subpixel land cover mixtures in coarse-resolution satellite data, *Remote Sensing of Environment*, 58:329–343.

NeuralWare, 1993. Reference Guide: Software Reference for Professional II/Plus and Neural Works Explorer, NeuralWare, Inc.

Roberts, D.A., M.O. Smith, and J.B. Adams, 1993. Green vegetation, non-photosynthetic vegetation, and soils in AVIRIS data, *Remote Sensing of Environment*, 44:222–269.

Settle, J., and N. Drake, 1993. Linear mixing and the estimation of ground cover proportions, *International Journal of Remote Sens*ing, 14:1159–1177.

Shimabukuro, Y.E., and J.A. Smith, 1991. The least squares mixing models to generate fraction images derived from remote sensing multispectral data, *IEEE Transactions on Geoscience and Remote Sensing*, 29:16–20.

Sohn, Y., and R.M. McCoy, 1997. Mapping desert shrub rangeland using spectral unmixing and modeling spectral mixture with TM data, *Photogrammetric Engineering & Remote Sensing*, 63: 707–716.

Strahler, A.N., C.E., Woodcock, and J.A. Smith, 1986. On the nature of models in remote sensing, *Remote Sensing of Environment*, 20:121–139.

Townshend, J.R.G., and C.O. Justice, 1981. Information extraction from remotely sensed data: a user view, *International Journal of Remote Sensing*, 2:313–329.

Wang, Y., and D.L. Civco, 1996. Three Artificial Neural Network Paradigms in Multisource Spatial Data Land Cover Classification, *Geographic Information Sciences*, 1:73–87.

Warner, T.A., and M. Shank, 1997. An evaluation of the potential for fuzzy classification of multispectral data using artificial neural networks, *Photogrammetric Engineering & Remote Sensing*, 63: 1285–1294.

Woodcock, C.E., S. Gopal, and W. Albert, 1996. Evaluation of the potential for providing secondary labels in vegetation maps, *Photogrammetric Engineering & Remote Sensing*, 62:393–399.

Woodcock, C.E., and A.H. Strahler, 1987. The Factor of Scale in Remote Sensing, *Remote Sensing of Environment*, 21:311–332.

(Received 04 September 2002; accepted 03 July 2003; revised 29 July 2003)